

DRAFT

CMS Paper

The content of this note is intended for CMS internal use and distribution only

2012/01/26

Head Id: 98703

Archive Id: 98707

Archive Date: 2012/01/27

Archive Tag: trunk

Search for Heavy Top-like Quark Pair Production in the Dilepton Final State in pp Collisions at $\sqrt{s} = 7$ TeV

The CMS Collaboration

Abstract

The results of a search for pair production of a heavy top-like quark, t' , in the decay mode $t'\bar{t}' \rightarrow bW^+\bar{b}W^- \rightarrow b\ell^+\nu\bar{b}\ell^-\bar{\nu}$ are presented. The search is performed in a data sample corresponding to a total integrated luminosity of 4.7 fb^{-1} of pp collisions at a centre-of-mass energy of 7 TeV, collected by the CMS experiment at the LHC. The observed number of events agrees with the expectation from standard model processes, and no evidence of $t'\bar{t}'$ production is found. Upper limits on the production cross section as a function of t' mass are presented. A t' with a mass below $552 \text{ GeV}/c^2$ is excluded at the 95% C.L.

This box is only visible in draft mode. Please make sure the values below make sense.

PDFAuthor: Yanjun Tu, Jacob Linacre, Frank Wuerthwein

PDFTitle: Search for Heavy Top-like Quark Pair Production in the Dilepton Final State in pp Collisions at $\sqrt{s}=7$ TeV

PDFSubject: CMS

PDFKeywords: CMS, physics, dilepton, top-like, tprime, fourth generation

Please also verify that the abstract does not use any user defined symbols

1 Introduction

Since the discovery of the top quark at the Tevatron, there have been many searches for a possible new generation of fermions. Those searches have not found evidence of new fermions beyond the standard model (SM). However, from a theoretical point of view, the number of generations of fermions is not limited to three. The extension of the generations of fermions may have a significant effect on neutrino physics, flavor physics and Higgs physics. A fourth generation of quarks, t' and b' , would allow indirect bounds on the Higgs boson mass to be relaxed [1, 2], and may possess enough intrinsic matter and anti-matter asymmetry to be relevant to the baryon asymmetry of the Universe [3]. Therefore, there is continued theoretical and experimental interest in such a fourth generation [4]. Previous direct searches restrict the masses of quarks in the fourth generation, $M_{t'}$ and $M_{b'}$, to be greater than 350 GeV/ c^2 [5, 6], and the indirect search from LEP excludes a fourth generation of light neutrinos [7]. At the LHC, the QCD production cross section of $t'\bar{t}'$ is expected to be two orders of magnitude larger than that at the Tevatron for $M_{t'} = 500$ GeV/ c^2 [8]. This brings us a great opportunity to explore the possibility of new physics with an extended generation of fermions.

We present a search for a heavy top-like quark in the final state $t' \rightarrow bW \rightarrow b\ell\nu$, using pair production of $t'\bar{t}'$ in pp collisions at a centre-of-mass energy of 7 TeV. This search is well motivated if $M_{t'} < M_{b'}$ or if $M_{t'} > M_{b'}$ and the mass splitting between t' and b' is less than M_W , which is favored by precision electroweak measurements [2, 9]. The dilepton $t'\bar{t}'$ search has a small SM background, and is hence a clean environment to search for new physics.

The search uses a data sample corresponding to a total integrated luminosity of 4.7 fb $^{-1}$ collected by the Compact Muon Solenoid (CMS) experiment at the LHC during 2011. A preliminary result of this search, using the first 1.1 fb $^{-1}$ of the total integrated luminosity, excluded a t' quark with a mass below 422 GeV/ c^2 at the 95% C.L. [10].

2 CMS Detector

The central feature of the CMS apparatus is a superconducting solenoid, 13 m in length and 6 m in diameter, which provides an axial magnetic field of 3.8 T. Within the field volume are several particle detection systems. Charged particle trajectories are measured by silicon pixel and silicon strip trackers, covering $0 \leq \phi \leq 2\pi$ in azimuth and $|\eta| < 2.5$ in pseudorapidity, defined as $\eta = -\log[\tan \theta/2]$, where θ is the polar angle of the trajectory of the particle with respect to the counterclockwise proton beam direction. A crystal electromagnetic calorimeter and a brass/scintillator hadronic calorimeter surround the tracking volume, providing energy measurements of electrons and hadronic jets. Muons are identified and measured in gas-ionization detectors embedded in the steel return yoke outside the solenoid. The detector is nearly hermetic, allowing energy balance measurements in the plane transverse to the beam direction. A two-tier trigger system selects the most interesting pp collision events for use in physics analysis. A more detailed description of the CMS detector can be found elsewhere [11].

3 Event Preselection

The data used for this measurement are collected using one of the ee , $e\mu$, or $\mu\mu$ high- p_T dilepton triggers. Muon candidates are reconstructed with two algorithms, one in which tracks in the silicon detector are matched to consistent signals in the calorimeters and muon system, and another in which a simultaneous fit is performed to hits in the silicon tracker and muon system [12]. Electron candidates are reconstructed starting from a cluster of energy deposits in

the electromagnetic calorimeter, which is then matched to hits in the silicon tracker. A selection using electron identification variables based on shower shape and track-cluster matching is applied to the reconstructed candidates [13]. Electron candidates within $\Delta R \equiv \sqrt{\Delta\phi^2 + \Delta\eta^2} < 0.1$ of a muon are rejected to remove candidates due to muon bremsstrahlung and final-state radiation. Both electrons and muons are required to be isolated from other activity in the event. This is achieved by imposing a maximum allowed value of 0.15 on I_{rel} , an observable defined as the ratio of the scalar sum of transverse track momenta and transverse calorimeter energy deposits within a cone of $\Delta R < 0.3$ around the lepton candidate direction at the origin, to the transverse momentum of the candidate. Events selected for the analysis are required to have two opposite-sign, isolated leptons (e^+e^- , $e^\pm\mu^\mp$, or $\mu^+\mu^-$). Both leptons must have $p_T > 20$ GeV/ c , and the electrons (muons) must have $|\eta| < 2.5$ ($|\eta| < 2.4$), and be consistent with originating from the same interaction vertex. In the rare case of events with more than two such leptons ($< 0.1\%$ of events), the two leptons with the highest p_T are selected. Events with an e^+e^- or $\mu^+\mu^-$ pair with invariant mass between 76 GeV/ c^2 and 106 GeV/ c^2 or below 12 GeV/ c^2 are removed, in order to suppress Drell-Yan events, $Z/\gamma^* \rightarrow \ell^+\ell^-$, as well as low mass dilepton resonances.

The jets and the missing transverse energy E_T^{miss} are reconstructed with the Particle Flow technique [14]. At least two jets with $p_T > 30$ GeV/ c and $|\eta| < 2.5$, separated by $\Delta R > 0.4$ from leptons passing the analysis selection, are required to be in the event. The anti- k_T clustering algorithm [15] with $\Delta R = 0.5$ is used for jet clustering. Exactly two of the jets are required to be consistent with coming from the decay of heavy flavor and be identified as b jets by the TCHEM b tagging algorithm described in Ref. [16], which relies on tracks with large impact parameters. The E_T^{miss} in the event is required to exceed 50 GeV.

Signal and background studies are performed using the simulated events generated by the MADGRAPH 4.4.12 [17] or PYTHIA 6.4.22 [18] event generators. The samples of $t'\bar{t}'$, $t\bar{t}$, Drell-Yan (DY) with $M_{\ell\ell} > 50$ GeV/ c^2 , di-boson (WW, WZ and ZZ only: the contribution from $W\gamma$ is assumed to be small), and single top events are generated using MADGRAPH. The samples of Drell-Yan events with $M_{\ell\ell} < 50$ GeV/ c^2 are generated using PYTHIA. They are then simulated using a GEANT4-based model [19] of the CMS detector, and finally reconstructed and analyzed using the same software as is used to process collision data. The cross section for $t\bar{t}$ production is taken from Ref. [20], while next-to-leading order (NLO) cross sections are used for the remaining SM background samples. The $t'\bar{t}'$ cross sections are calculated to approximate NNLO using HATHOR [21].

Due to the varying LHC luminosity, the mean number of interactions in a single beam crossing increased over the course of data taking up to ~ 15 near the end of the 2011 data taking period. In the following, the yields of simulated events are weighted such that the distribution of reconstructed vertices observed in data is reproduced. The efficiency for events containing two leptons satisfying the analysis selection to pass at least one of the double-lepton triggers is measured to be approximately 100%, 95%, and 90% for the ee , $e\mu$, and $\mu\mu$ triggers respectively [22], and corresponding weights are applied to the simulated event yields. In addition, b tagging scale factors are applied to simulated events for each jet, due to the difference of b tagging efficiencies between data and simulation [16].

The observed and simulated yields after the above event preselection are listed in Table 1, in which $t\bar{t} \rightarrow \ell^+\ell^-$ and $\text{DY} \rightarrow \ell^+\ell^-$ correspond to dileptonic $t\bar{t}$ and DY decays, including tau leptons. All other $t\bar{t}$ decay modes are included in $t\bar{t} \rightarrow \text{fake}$. The yields are dominated by top-pair production in the dilepton final state, and reasonable agreement is observed between data and simulation. The expected yields from $t'\bar{t}'$ are also shown for different values of $M_{t'}$.

Table 1: The observed and simulated yields after the preselection described in the text, for an integrated luminosity of 4.7 fb^{-1} . Uncertainties are statistical only, and the systematic uncertainties on the simulated yields are given in Section 6. Where the simulated yields are zero, upper limits are given based on the weighted yield if one of the simulated events had passed selection.

Sample	ee	$\mu\mu$	$e\mu$	all
$t'\bar{t}', M_{t'} = 400 \text{ GeV}/c^2$	10.0 ± 0.9	13.0 ± 1.0	27.7 ± 1.4	50.7 ± 1.9
$t'\bar{t}', M_{t'} = 500 \text{ GeV}/c^2$	2.8 ± 0.2	3.1 ± 0.2	6.3 ± 0.3	12.2 ± 0.5
$t'\bar{t}', M_{t'} = 600 \text{ GeV}/c^2$	0.8 ± 0.1	1.0 ± 0.1	2.1 ± 0.1	3.9 ± 0.2
$t\bar{t} \rightarrow \ell^+\ell^-$	494.2 ± 11.2	622.3 ± 12.1	1490.7 ± 19.1	2607.2 ± 25.3
$t\bar{t} \rightarrow \text{fake}$	7.3 ± 1.4	0.5 ± 0.3	10.7 ± 1.6	18.4 ± 2.1
W + jets	< 1.8	< 1.8	< 1.8	< 1.8
$\text{DY} \rightarrow \ell^+\ell^-$	2.7 ± 1.4	1.5 ± 0.9	0.5 ± 0.5	4.8 ± 1.7
Di-boson	0.5 ± 0.1	1.0 ± 0.1	1.8 ± 0.2	3.3 ± 0.3
Single top	14.7 ± 0.9	18.3 ± 1.0	44.1 ± 1.6	77.1 ± 2.1
Total Background	519.4 ± 11.4	643.6 ± 12.2	1547.8 ± 19.3	2710.9 ± 25.5
Data	510	615	1487	2612

4 Signal Region

After preselection, the sample is dominated by SM $t\bar{t}$ events. Since a t' quark is expected to have a much larger mass than the top quark, variables that are correlated to the decaying quark mass can help distinguish $t'\bar{t}'$ events from $t\bar{t}$ events.

The masses of lepton and jet (M_{lb}), from the t/t' and \bar{t}/\bar{t}' decays, are chosen for this purpose. At generator level, all $t\bar{t}$ events have M_{lb} less than $\sqrt{M_t^2 - M_W^2}$, while most of the $t'\bar{t}'$ events have M_{lb} larger than that value. At reconstruction level, there are two ways to combine the two leptons and two b jets in each event, giving four possible values of M_{lb} . The minimum value of the four masses ($M_{\text{lb}}^{\text{min}}$) is found to be a good variable to distinguish the signal events from $t\bar{t}$ events.

Following these observations, the signal region is defined by adding the requirement of the minimum mass of lepton and jet pairs to the preselection: $M_{\text{lb}}^{\text{min}} > 170 \text{ GeV}/c^2$. This additional selection reduces the expected number of $t\bar{t}$ events by four orders of magnitude compared to the preselection prediction of Table 1. The simulated yields of $t'\bar{t}'$ events are typically reduced by 50%, and are given for different values of $M_{t'}$ in Table 2.

Table 2: The expected yields of $t'\bar{t}'$ events in the signal region for different values of $M_{t'}$, for an integrated luminosity of 4.7 fb^{-1} . Uncertainties are statistical only.

Sample	ee	$\mu\mu$	$e\mu$	all
$t'\bar{t}', M_{t'} = 400 \text{ GeV}/c^2$	3.28 ± 0.48	5.14 ± 0.60	10.49 ± 0.87	18.91 ± 1.16
$t'\bar{t}', M_{t'} = 500 \text{ GeV}/c^2$	1.36 ± 0.16	1.82 ± 0.18	3.15 ± 0.23	6.32 ± 0.33
$t'\bar{t}', M_{t'} = 600 \text{ GeV}/c^2$	0.53 ± 0.06	0.56 ± 0.06	1.25 ± 0.09	2.34 ± 0.12

5 Background Estimation

One of the main causes of background events appearing in the signal region is the misidentification of b jets and leptons. A misidentified lepton is defined as a lepton candidate not originating from an electroweak decay, such as a lepton from semileptonic b or c decays, a muon decay-in-flight, a pion misidentified as an electron, or an unidentified photon conversion. Misidentified b jets are referred to as “mistags”, and occur when a non-b jet is mistakenly b tagged.

The background events in the signal region can be divided into the following categories:

- Category I: events with mistagged b(s) and 2 real leptons
- Category II: events with misidentified lepton(s) and 2 real bs
- Category III: events with 2 real bs and 2 real leptons
- Category IV: events with mistagged b(s) and misidentified lepton(s).

To predict the number of events with mistagged b(s) (Category I), control regions in data are used where events pass all selection requirements except the number of b tagged jets. The number of background events with one mistag, $N_{1\text{-mistag}}$, is estimated from events with 1 b tag. Each event is weighted based on the mistag rate m_i for each untagged jet in the event, where m_i gives the p_T - and η -dependent probability for non-b jet i to be b tagged [16]. Where there are no untagged jets passing selection the event weight is zero, and for each untagged jet i passing selection the event weight is increased by $m_i / (1 - m_i)$. A similar calculation is made using events with 0 b tags to estimate the number of events with 2 mistags, $N_{2\text{-mistags}}$. This time a weight of $\frac{m_i}{1-m_i} \times \frac{m_j}{1-m_j}$ is used for each pair of untagged jets passing selection, where m_i and m_j are the mistag rates for the two untagged jets. The final prediction is obtained from $N_{\text{mistags}} = N_{1\text{-mistag}} - N_{2\text{-mistags}}$, which takes into account that $N_{2\text{-mistags}}$ is counted twice in $N_{1\text{-mistag}}$. The performance of the method is checked using simulated events, and an under-prediction of up to 50% is observed. Thus, a 100% systematic uncertainty is assigned to the prediction. In data, the predicted number of events with mistags in the signal region is $N_{\text{mistags}} = 0.74 \pm 0.27 \pm 0.74$, where the uncertainties are statistical and systematic respectively. The expected Category I yield from simulation, taken as a cross-check, is 0.98 ± 0.34 , and is in reasonable agreement.

The background from events with misidentified leptons (Category II) is predicted based on the number of events in data with a candidate lepton that can only pass loosened selection criteria [23]. Using a measurement of the fraction of such “loose” leptons that go on to pass the selection cuts, the number of misidentified leptons in the event sample can be estimated. However, there are no events in data where one or more of the lepton candidates passes only the loosened selection criteria, resulting in a prediction of $0_{-0.0}^{+0.4}$ events where the upper uncertainty corresponds to the prediction of the method had there been one such event. The Category II event yield is also zero in simulation.

Simulation is used to predict the number of events with no misidentified bs or leptons (Category III). Selecting only events where both bs and leptons are well matched to the corresponding particles at generator level, the resulting prediction is 0.99 ± 0.69 where the uncertainty is statistical only.

The contribution of events from Category IV is assumed to be negligible and is covered by both the Category I and Category II predictions. Since the Category II prediction is zero no double-counting can have occurred.

6 Systematic Uncertainties

The systematic uncertainty of the signal acceptance is dominated by the uncertainty on the b tagging efficiency. The uncertainty is 15% for b jets with $p_T > 240$ GeV/c, and 4% for b jets with $p_T \leq 240$ GeV/c [16]. Other uncertainties are assessed on the trigger efficiency (2%) [22], lepton selection (2%) [22], and jet and E_T^{miss} energy scale (8%) [24]. These four sources combine to a 19% relative uncertainty on the signal Acceptance \times Efficiency, and there is a further 4.5% uncertainty on the luminosity [25].

The systematic uncertainty of the background estimate is dominated by the uncertainty on the data driven estimate of events with mistagged b jets (100%), and the lack of selected events in the loose-lepton control region. The systematic uncertainties on these sources of background are included in the summary of background predictions in Table 3.

7 Results and Conclusions

The number of expected events from SM background processes is 1.73 ± 1.12 , and one event is observed in the $e\mu$ channel. There is thus no evidence for an excess of events above SM expectations. A summary of the observed and predicted yields is presented in Table 3.

The simulated distribution of $M_{\text{lb}}^{\text{min}}$ from SM background processes is compared to the data in Figure 1, where the expected distribution for a $t'\bar{t}'$ signal with $M_{t'} = 450$ GeV/ c^2 is also shown. The simulated background yields in the signal region are scaled so that they match the yields estimated from control regions in data given in Table 3, and outside the signal region the simulated background yields are taken without rescaling.

Table 3: Summary of the predicted background yields and the observation in data. Uncertainties include both statistical and systematic errors, apart from Category III where the uncertainty is statistical only.

Sample	Yield
Category I (data-driven)	0.74 ± 0.79
Category II (data-driven)	$0^{+0.4}_{-0.0}$
Category III (simulated)	0.99 ± 0.69
Total prediction	1.73 ± 1.12
Data	1

Since no excess beyond the SM background is found, 95% C.L. upper limits on the production cross section of $t'\bar{t}'$ as a function of t' mass are set, using the CL_s method [26, 27].

The limit calculation is based on the information provided by the observed event count combined with the values and the uncertainties of the luminosity measurement, the background prediction, and the fraction of all $t'\bar{t}'$ events expected to be selected. This fraction is the Efficiency \times Acceptance \times Branching Ratio for simulated signal events, and is given in Table 4 for different values of $M_{t'}$.

The calculated limits are shown in Figure 2 and Table 5. In conclusion, the expected and observed 95% C.L. lower bounds on the t' mass are 542 GeV/ c^2 and 552 GeV/ c^2 respectively from the analysis of a data sample corresponding to an integrated luminosity of 4.7 fb^{-1} .

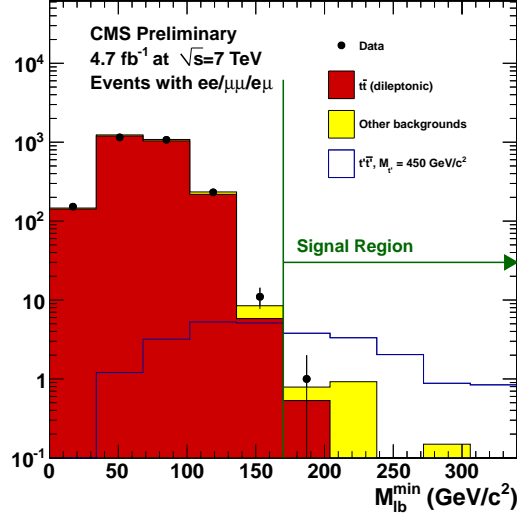


Figure 1: Comparison of data and the simulated background for M_{lb}^{\min} . The signal region is defined by $M_{lb}^{\min} > 170$ GeV/ c^2 . The simulated background yields in the signal region are scaled so that they match the yields estimated from control regions in data given in Table 3, and outside the signal region the simulated background yields are taken without rescaling. One data event is observed in the signal region. The expected distribution for a $t'\bar{t}'$ signal is also shown for $M_{t'} = 450$ GeV/ c^2 .

Table 4: Efficiency \times Acceptance \times Branching Ratio in simulated events for different t' masses. Each value has a relative uncertainty of 19%.

Sample	Eff \times Acc \times BR
$t'\bar{t}', M_{t'} = 350$ GeV/ c^2	0.16%
$t'\bar{t}', M_{t'} = 400$ GeV/ c^2	0.29%
$t'\bar{t}', M_{t'} = 450$ GeV/ c^2	0.35%
$t'\bar{t}', M_{t'} = 500$ GeV/ c^2	0.41%
$t'\bar{t}', M_{t'} = 550$ GeV/ c^2	0.48%
$t'\bar{t}', M_{t'} = 600$ GeV/ c^2	0.54%

References

- [1] P. Q. Hung and M. Sher, “Experimental constraints on fourth generation quark masses”, *Phys. Rev. D* **77** (Feb, 2008) 037302. doi:10.1103/PhysRevD.77.037302.
- [2] G. D. Kribs, T. Plehn, M. Spannowsky et al., “Four generations and Higgs physics”, *Phys. Rev. D* **76** (Oct, 2007) 075016. doi:10.1103/PhysRevD.76.075016.
- [3] W.-S. Hou, “CP violation and baryogenesis from new heavy quarks”, *Chin. J. Phys.* **47** (2009) 134, arXiv:0803.1234.
- [4] B. Holdom et al., “Four statements about the fourth generation”, *PMC Phys.* **A3** (2009) 4, arXiv:0904.4698. doi:10.1186/1754-0410-3-4.

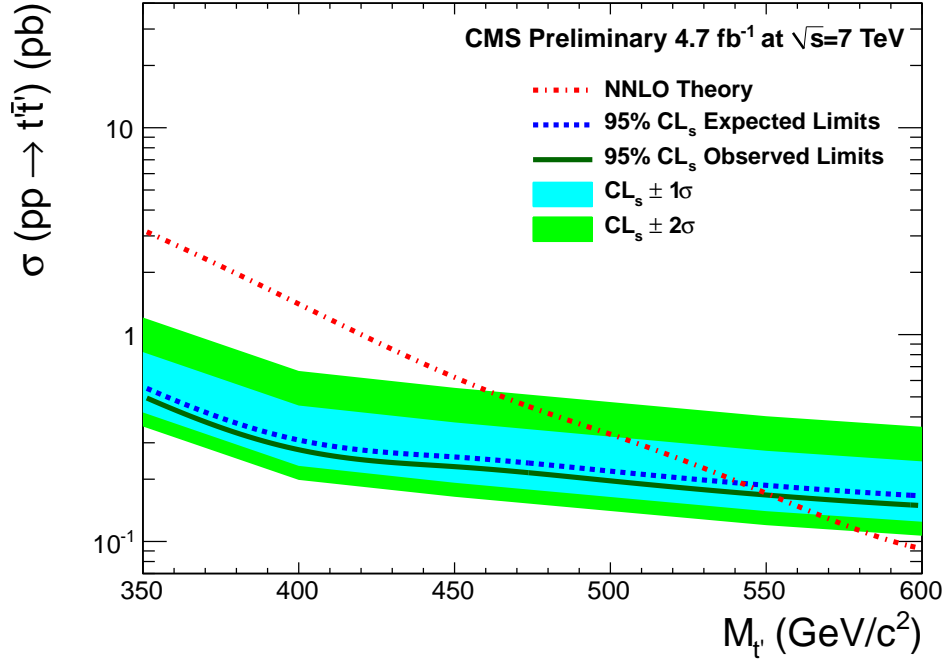


Figure 2: The 95% C.L. upper limits on the production cross section of $t'\bar{t}'$ as a function of t' mass are shown. The expected 95% C.L. lower bound on $M_{t'}$ is 542 GeV/c^2 and the observed 95% C.L. lower bound on $M_{t'}$ is 552 GeV/c^2 .

Table 5: The approximate NNLO theoretical cross section of $t'\bar{t}'$ production [21] and the 95% C.L. upper limits on the production cross section of $t'\bar{t}'$.

$M_{t'}$	350 GeV/c^2	400 GeV/c^2	450 GeV/c^2	500 GeV/c^2	550 GeV/c^2	600 GeV/c^2
Theory (pb)	3.200	1.406	0.622	0.330	0.171	0.092
Expected (pb)	0.560	0.309	0.256	0.219	0.187	0.166
Observed (pb)	0.503	0.278	0.230	0.196	0.168	0.149

[5] The CDF Collaboration, “Search for a heavy top-like quark in $p\bar{p}$ collisions at $\sqrt{s} = 1.96$ TeV”, *Phys. Rev. Lett.* **107** (2011) 261801, arXiv:1107.3875. doi:10.1103/PhysRevLett.107.261801.

[6] The CDF Collaboration, “Search for heavy bottom-like quarks decaying to an electron or muon and jets in $p\bar{p}$ collisions at $\sqrt{s} = 1.96$ TeV”, *Phys. Rev. Lett.* **106** (2011) 141803, arXiv:1101.5728. doi:10.1103/PhysRevLett.106.141803.

[7] D. Decamp et al., “Determination of the number of light neutrino species”, *Phys. Lett. B* **231** (1989) 519.

[8] E. L. Berger and Q.-H. Cao, “Next-to-leading order cross sections for new heavy fermion production at hadron colliders”, *Phys. Rev. D* **81** (2010) 035006, arXiv:0909.3555. doi:10.1103/PhysRevD.81.035006.

- [9] O. Eberhardt, A. Lenz, and J. Rohrwild, “Less space for a new family of fermions”, *Phys. Rev. D* **D82** (2010) 095006, [arXiv:1005.3505](#).
doi:10.1103/PhysRevD.82.095006.
- [10] CMS Collaboration, “Search for a heavy top-like quark in the dilepton final state in pp Collisions at $\sqrt{s} = 7$ TeV”, *CMS Physics Analysis Summary* **CMS-PAS-EXO-11-050** (2011).
- [11] CMS Collaboration, “The CMS experiment at the CERN LHC”, *JINST* **3** (2008) S08004.
- [12] CMS Collaboration, “Performance of muon identification in pp collisions at $\sqrt{s} = 7$ TeV”, *CMS Physics Analysis Summary* **CMS-PAS-MUO-10-004** (2011).
- [13] CMS Collaboration, “Electron reconstruction and identification at $\sqrt{s}=7$ TeV”, *CMS Physics Analysis Summary* **CMS-PAS-EGM-10-004** (2010).
- [14] CMS Collaboration, “Commissioning of the particle-flow reconstruction in minimum-bias and jet events from pp collisions at 7 TeV”, *CMS Physics Analysis Summary* **CMS-PAS-PFT-10-002** (2010).
- [15] M. Cacciari, G. Salam, and G. Soyez, “The anti- k_T jet clustering algorithm”, *Journal of High Energy Physics* **2008** (2008), no. 04, 063.
- [16] CMS Collaboration, “Commissioning of b-jet identification with pp collisions at $\sqrt{s} = 7$ TeV”, *CMS Physics Analysis Summary* **CMS-PAS-BTV-11-003** (2011).
- [17] J. Alwall et al., “MadGraph/MadEvent v4: the new web generation”, *JPHYS* **31** (2005) N9–N20.
- [18] T. Sjöstrand, S. Mrenna, and P. Skands, “PYTHIA 6.4 physics and manual”, *JHEP* **05** (2006) 026.
- [19] S. Agostinelli et al., “GEANT4 – a simulation toolkit”, *Nucl. Instr. and Methods A* **506** (2003) 250–303.
- [20] CMS Collaboration, “Combination of top pair production cross section measurements”, *CMS Physics Analysis Summary* **CMS-PAS-TOP-11-024** (2011).
- [21] M. Aliev et al., “HATHOR, hadronic top and heavy quarks cross section calculator”, *Comput. Phys. Commun.* **182** (2011) 1034.
- [22] CMS Collaboration, “Search for physics beyond the Standard Model in opposite-sign dilepton events at $\sqrt{s} = 7$ TeV”, *CMS Physics Analysis Summary* **CMS-PAS-SUS-11-011** (2011).
- [23] CMS Collaboration, “Search for new physics with same-sign isolated dilepton events with jets and missing transverse energy at the LHC”, [arXiv:1104.3168v1](#).
- [24] CMS Collaboration, “Determination of the jet energy scale in CMS with pp collisions at $\sqrt{s} = 7$ TeV”, *CMS Physics Analysis Summary* **CMS-PAS-JME-10-010** (2010).
- [25] CMS Collaboration, “Measurement of CMS luminosity”, *CMS Physics Analysis Summary* **CMS-PAS-EWK-10-004** (2010).
- [26] T. Junk, “Confidence level computation for combining searches with small statistics”, *Nucl. Instrum. Meth.* **362** (1999) 435.
- [27] A. L. Read, “Presentation of search results: the CL_s technique”, *J. Phys. G* **28** **364** (2002) 2693.